

Causal Discovery from Sparse Time-Series Data Using Echo State Network

Haonan Chen^{†1}, Bo Yuan Chang^{†1}, Mohamed A. Naiel¹,
Georges Younes¹, Steven Wardell², Stan Kleinikkink², and John S. Zelek¹

¹ Vision and Image Processing Group,
University of Waterloo, Waterloo, ON, Canada
{haonan.chen,by2chang, mohamed.naiel, georges.younes,
jzelek}@uwaterloo.ca

² ATS Automation, Cambridge, ON, Canada
{swardell, skleinikkink}@atsautomation.com

**

Abstract. Causal discovery between collections of time-series data can help diagnose causes of symptoms and hopefully prevent faults before they occur. However, reliable causal discovery can be very challenging, especially when the data acquisition rate varies (*i.e.*, non-uniform data sampling), or in the presence of missing data points (*e.g.*, sparse data sampling). To address these issues, we propose a new system comprised of two parts, the first part fills missing data with a Gaussian Process Regression, and the second part leverages an Echo State Network, which is a type of reservoir computer (*i.e.*, used for chaotic system modelling) for Causal discovery.

We evaluate the performance of our proposed system against three other off-the-shelf causal discovery algorithms, namely, structural expectation maximization, sub-sampled linear auto-regression absolute coefficients, and multivariate Granger Causality with vector auto-regressive using the Tennessee Eastman chemical dataset; we report on their corresponding Matthews Correlation Coefficient (MCC) and Receiver Operating Characteristic curves (ROC) and show that the proposed system outperforms existing algorithms, demonstrating the viability of our approach to discover causal relationships in a complex system with missing entries.

Keywords: Time-series causality · Echo State Network · Sparsely Sampled Data · Gaussian Process Regression

1 Introduction

Artificially replicating and surpassing human’s ability to interpret causal relationships is considered an evolutionary step forward when compared to existing Artificial Intelligence systems [1]. Despite several decades of research, current state-of-the-art deep learning systems are still broadly interpreted as a family of highly nonlinear statistical models [2] or pattern detection regression engines that require a very large set of

**[†] Equal contribution.

training samples to distill a meaningful outcome for a particular problem. In contrast, humans are capable of drawing conclusions and solving problems by identifying causal relationships between the different variables of a task using a very small amount of data. This inspired a large body of researchers to work on causal discovery algorithms in an attempt to answer various challenges in several fields, such as epidemiology [3], economy [4, 5], and medicine [6] to name a few. However, due to the complex relationships between a large number of hidden variables, learning causal relationships on real-world data can be very challenging as causality must be inferred from noisy data [7, 8]. Moreover, it is not uncommon to run into missing values when working with real-world data, especially when hardware limitations and human errors play an important factor in the data acquisition process (*e.g.*, time series data).

Causal discovery in time-series data is of particular importance in this work as we attempt to retrieve causal relationships from sparsely sampled time-series data. Despite the existence of several methods for causal discovery [9–11], there is currently a limited availability for methods that address causal discovery from *sparse* time-series data. While the effects of missing data points from a sparsely sampled sequence can be often solved with hardware upgrades, or better training for the employees, such solutions are often associated with a steep price tag and can be time consuming. Alternatively, one could make use of data filling interpolation methods to populate the sparse time-series sequence before performing causal learning as in [12]. To that end, we propose a system that makes use of Gaussian Process Regression (GPR) to fill missing data points, which are in turn processed with an Echo State network tailored to the causal discovery of relationships between its nodes.

2 Related Work

Existing time-series causality algorithms can be broadly categorized into five main groups as shown in Fig. 1, namely, classical time-series approaches [13], chaos and dynamic systems approaches [14], information theoretic approaches [15], graphical approaches [16], and finally machine learning approaches [17]. We briefly touch upon these topics and discuss some of their limitations in what follows, the interested reader is referred to the original publication for further details [13–17].

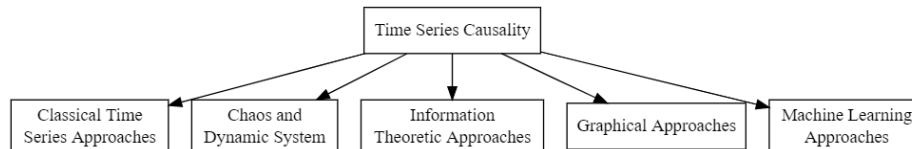


Fig. 1: Taxonomy of Time-Series Causal Discovery

Classical time-series approaches are widely adopted for dealing with time-series causality. Within this classical framework, there are several ways researchers can examine Granger Causality such as vector autoregressive model (VAR in short) [18], Pearson

Correlations [19], F-test[20] and Toda and Yamamoto Procedure [21], *etc.* While these methods are generally intuitive and easy to implement, they struggle to identify complicated non-linear causal relationships.

Chaos and Dynamic approaches share many similarities with *Information Theoretic approaches*. Methods that can be classified under these frameworks and are used to examine linear and non-linear Granger Causality include the Hiemstra-Jones test [22], Convergent cross mapping (CCM) [23], and Transfer Entropy (TE) measure [24]. While these two categories are capable of handling non-linear relationships, they can be difficult to implement due to their constraints and requirements [25] [26].

Graphical Approaches model Granger Causality in a multivariate setting by representing each variable as a node on a graph, with Granger Causality represented as directed edges between the nodes. Some methods under the graphical approach take into consideration of the probabilistic element into causal relationships where the causal effect is a probability rather than a certainty. Some of the methods under graphical approaches include [27], Expectation Maximization (EM) [28], and Structural Expectation Maximization (SEM) [29]; an interesting survey for applications that fall under this category can be found at [30]. In general, the causal prediction accuracy of graphical approaches is somewhat inconsistent and depends heavily on the manual fine tuning of hyper-parameters.

Finally, *Machine Learning* (ML) is a new area that researchers are currently exploring for causal discovery. Recent machine learning methods include Attention-Based Convolutional Neural Network (ABCNN) approach [10] and Echo State Network approach [31]. There are many advantages favoring ML based algorithm over the other approaches, for example they can handle relatively large and complicated data, they require less human intervention for tuning, they can be adaptable to a wide range of applications, and they are backed by a largely motivated support and development community [32]. While there are several drawbacks to ML methods such as the expensive compute cost and the relatively long training time, the advantages outweigh the disadvantages and hence we adopt in this work a ML based algorithm for causal discovery.

3 System Model

Despite the large number of solutions put forward in the literature, most time-series algorithms build upon the same Granger Causality [13] concepts which state:

1. Only the input/intervention from the past can Granger cause the outcome in the future, *i.e.* future input/intervention cannot Granger cause any past values.
2. Having information about variable A can improve the predictability of variable B .

When the two conditions are met then one can say that variable A Granger Causes variable B (and vice versa).

Under the above assumptions, let a time-varying system comprised of n time-series be defined as $\mathcal{S} = \{T_1(t), T_2(t), \dots, T_n(t)\}$, where $T_i(t)$ represents the i^{th} time-series component of the system; then one can state $T_i(t)$ Granger causes $T_j(t)$, for $T_i, T_j \in \mathcal{S}$ if and only if:

$$\mathcal{P} [T_i(t+1) | \mathcal{I}(T(t))] \neq \mathcal{P} [T_i(t+1) | \mathcal{I} (T^{(-j)}(t))] \quad (1)$$

Where \mathcal{P} is the probability density function and $\mathcal{I}(T^{(-j)}(t))$ represents all the usable information provided by the time-series system up to time t excluding the j^{th} component [33].

To perform causal learning with missing values, we propose a two part solution: (1) data filling with Gaussian Process Regression, (3.2) and (2) causal learning with Granger Causality (GC) based Echo State Network (3.3).

3.1 Architecture

Our proposed approach is summarized in Fig. 2 where T is a time-series input with some missing data, T^* represents the multivariate time-series that was data-filled by GPR, and $GC(x_i, x_j)$ is the causal relation between x_i and x_j . The input is a $N \times M$ multivariate time-series where N is the total number of entries for each variable (feature) and M is the number of variables. The GPR filled time-series is then processed through the GC-ESN estimator (dynamic reservoir), to generate an $M \times M$ causality matrix, which can then be displayed as a heat map of causal relations amongst variables.

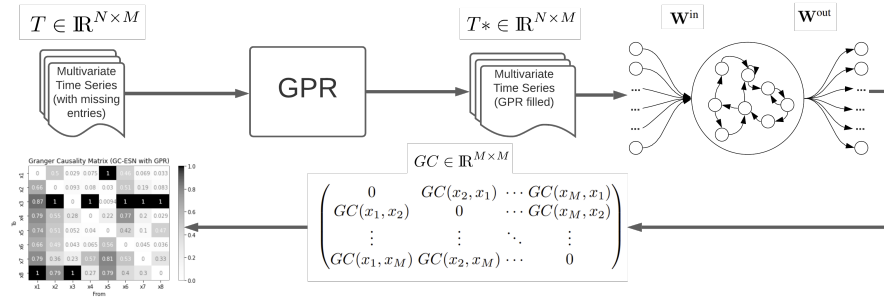


Fig. 2: Workflow of the proposed solution; a time-series with missing data is filled using GPR and fed into a GC-ESN to predict causal relations.

3.2 Gaussian Process Regression

To fill out the missing data we opt to use a non-parametric approach known as Gaussian Process Regression (GPR for short). Gaussian Process can be interpreted from two different views [34], namely the weight-space view and the function-space view. To limit the scope of this work, we restrict our discussion to GP's function-space interpretation, its associated hyper-parameters and GP's sampling techniques. For more details about GPR the reader is referred to [34], and to [12] for a filling performance comparison between GPR and dummy filling.

Function-Space View: GP defines a distribution over multiple functions (as opposed to finding a best fit with one function), that is, sampling two (or more) points from a function that follows a joint multivariate Gaussian distribution [35]. Since the sampled points can vary in time, the generated functions will change accordingly. In this interpretation, the Gaussian process is defined as a collection of a finite number of random variables that follow a joint Gaussian distribution. The Gaussian Process regression can be re-written into a form similar to that of linear regression:

$$y = f(x) + \epsilon, \quad (2)$$

where the noise term $\epsilon \sim \mathcal{N}(0, \sigma_\epsilon^2)$, reflects observation randomness. The Gaussian Process can then be defined by its mean function and co-variance matrix function, which can be written as:

$$f(x) \sim GP(m(x), k(x, x')), \quad (3)$$

where $m(x)$ is the mean function and $k(x, x')$ is the co-variance function (also known as the kernel function [36]) for the randomly selected two points x and x' . In turn (3) can be expanded such that:

$$m(x) = \mathbb{E}[f(x)], \text{ and} \quad (4)$$

$$k(x, x') = \mathbb{E}[(f(x) - m(x))(f(x') - m(x'))]. \quad (5)$$

There are many kernel functions to choose from and the choice is typically based on a priori knowledge of the data; for example, will variable b be affected when variable a is larger, and if so to what degree *etc.*). Other factors such as smoothness and the cycle patterns of the observed values can also influence the choice of the kernel function.

Hyper-Parameter-Based Kernels: One of the many advantages of GPR filling is its flexibility to incorporate a wide range of kernel functions that can be tailored to the working data. Different kernels have different hyper-parameters, that are typically fine-tuned to fit the working data via an iterative trial-and-error process, until a best fit is achieved. Usually the selection of hyper-parameter values is an iterative process for user should test out values before finding the most optimal values that can best represent the working dataset.

Sampling From GP: Once the mean and kernel functions (along with their associated hyper-parameters) are selected, the GP can then be used to sample data from the kernel functions. Without going into the derivation details, the sampling functions $f(x^*)$ can in turn be sampled from:

$$m_t(x) = K(X^*, x_t)[K(x_t, x_t) + \sigma_\epsilon^2 \mathbf{I}]^{-1} y_t, \text{ and} \quad (6)$$

$$k_t(x, x') = K(X^*, X^*) - K(X^*, x_t)K(X^*, x_t)^{-1}K(x_t, X^*), \quad (7)$$

where x_t is the value at instant t drawn from the master matrix that contains all the input points, X^* , and \mathbf{I} is the identity matrix. Just as in [37], the term X^* is represented as:

$$K(X^*, X^*) = \begin{pmatrix} k(x_1^*, x_1^*) & k(x_1^*, x_2^*) & \cdots & k(x_1^*, x_n^*) \\ k(x_2^*, x_1^*) & k(x_2^*, x_2^*) & \cdots & k(x_2^*, x_n^*) \\ \vdots & \vdots & \ddots & \vdots \\ k(x_n^*, x_1^*) & k(x_n^*, x_2^*) & \cdots & k(x_n^*, x_n^*) \end{pmatrix}, \quad (8)$$

where $k(x_1^*, x_2^*)$ is the kernel function constructed using the points x_1^* and x_2^* selected from X^* which contains all input values.

For detailed derivations of the above, the reader is referred to [37] and [34].

3.3 Granger Causality-Based Echo State Network

In this work we opt to use a special type of Recurrent Neural Networks (RNNs) known as an Echo State Network (ESN) [31] (also called Reservoir Computing and is typically used for chaotic system modelling) for causal discovery. Compared to traditional RNNs, ESNs train much faster as the weights of an ESN are randomly initialized and fixed during both training and inference. The ESN's output layer acts like a linear regressor thus providing much more flexibility to the ESN than the general RNN architecture. However, due to the non-linear nature of each unit's activation function, the model is able to capture non-linear causality with a much faster speed than the traditional RNN. The basic structure of an ESN is shown in Fig. 3, where the inputs are propagated

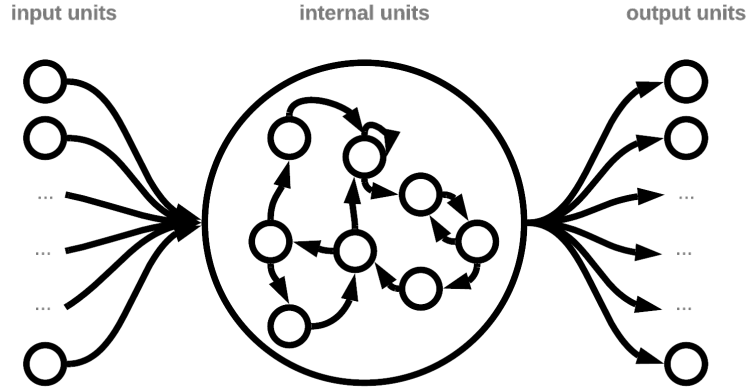


Fig. 3: Echo State Network Neurons Structure [31]

through the input layer and into the reservoir (the Internal Units). The Internal Units are randomly connected and their weights are fixed after kernel initialization [31].

Let $x(t)$ be the n^{th} internal unit, then during training, an update is computed according to

$$\mathbf{x}(t+1) = \mathbf{f}^{\text{out}}(\mathbf{W}^{\text{in}}\mathbf{u}(t+1) + \mathbf{W}\mathbf{x}(t) + \mathbf{W}^{\text{out}}\mathbf{y}(t)), \quad (9)$$

where $\mathbf{u}(t)$, $\mathbf{x}(t)$, $\mathbf{y}(t)$ represent the input, internal and output units at a time step t respectively. \mathbf{W}^{in} , \mathbf{W} and \mathbf{W}^{out} are their corresponding weight matrices. During training, \mathbf{W}^{in} During inference, the weights are fixed and the output is computed using:

$$\mathbf{y}(t+1) = \mathbf{f}^{\text{out}}(\mathbf{W}^{\text{out}}[\mathbf{u}(t+1); \mathbf{x}(t+1); \mathbf{y}(t)]), \quad (10)$$

where \mathbf{f}^{out} is the output function and $\mathbf{W}^{\text{out}} \in \mathbb{R}^{1 \times (1+M+L)}$ given a reservoir size M and input size L .

In this work, we follow the approach presented in [33], that is we model the ESN's reservoir units with an often used short-term memory term α and a variation term of the internal unit function [33, 38] $\tilde{\mathbf{x}}$ as:

$$\mathbf{x}(t) = (1 - \alpha)\mathbf{x}(t-1) + \alpha\tilde{\mathbf{x}}(t). \quad (11)$$

To model non-linear data, $\tilde{\mathbf{x}}$ is used since it is a linear combination of the input units $\mathbf{W}^{\text{in}}\mathbf{u}(t)$ and the previous reservoir states $\mathbf{W}\mathbf{x}(t-1)$, and is computed using:

$$\tilde{\mathbf{x}}(t) = f(\mathbf{W}^{\text{in}}[1; \mathbf{u}(t)] + \mathbf{W}\mathbf{x}(t-1)). \quad (12)$$

Note that the choice of α can have a large impact on the system's performance [31]. We then add an extended state $\mathbf{z}(t)$ which contains \mathbf{x} and \mathbf{u} [33]:

$$\mathbf{z}(t) = [1; \mathbf{x}(t); \mathbf{u}(t)] \quad (13)$$

given a reservoir size of M , we are then able to find the expected value of $u_i(t+1) | \mathcal{I}(\mathbf{u}(t))$:

$$E[u_i(t+1) | \mathcal{I}(\mathbf{u}(t))] = \mathbf{W}^{\text{out}}\mathbf{z}(t) \quad (14)$$

Eventually, we can find the ES-GC strength of j Granger causes i using the i -th squared residuals, $\varepsilon_i(t)$:

$$\varepsilon_i(t) = u_i(t+1) - \mathbf{W}^{\text{out}}\mathbf{z}(t) \quad (15)$$

the ES-GC strength of feature j causes i , $\text{GC}_{j \rightarrow i}$ is described as follow:

$$\text{GC}_{j \rightarrow i} = \log(\varepsilon^{-j} / \varepsilon_i) \quad (16)$$

4 Experiments and Evaluation

4.1 Dataset Description

We evaluate our proposed system on the Tennessee Eastman's Process Dataset (or TE for short) [39]. TE is a dataset that simulates actual chemical processes, and has been widely applied in the study of fault diagnosis and root cause analysis [40] [41]. The process flow consists of 5 major physical components: the reactor, condenser, vapor-liquid separator, compressor, and the product stripper. There are several sensor measurements available (such as flow rate, temperature, pressure and feed rate) for each components. Overall, the TE dataset contains 500 operation cycles' measurement from 52 sensor readings. Each operation cycle consists of 500 entries being recorded every 3 minutes

for a total duration of 1500 minutes. For further information about the TE dataset, the interested reader is referred to [42].

We select 8 sensors readings from the first 200 operation cycle’s entry inside the training fault free file for our experiment. The description for the 8 selected variables are shown in Table 1. In the the experimental procedure, we aim to recover these causal relationships and compare against their ground truth values.

Table 1: Selected Sensor’s Descriptions

Variable ID	Header in data	Description	Units
1	xmeas_5	Recycle Flow	km ³ /h
2	xmeas_6	Reactor feed rate	km ³ /h
3	xmeas_7	Reactor Pressure	kPa
4	xmeas_8	Reactor Level	%
5	xmeas_9	Reactor Temperature	°C
6	xmeas_12	Separator Level	%
7	xmeas_20	Compress Work	KW
8	xmeas_21	Reactor cooling water Outlet Temperature	°C

4.2 Experimental Setup

The selected TE data is first contaminated by removing 10% of its original entries. This provides ground truth data to validate the success of our proposed data filling process. Figure 4 shows the original vs. filled data for sensor 5 (recycling flow rate measurement).

The contaminated data is then processed through the proposed GPR method to fill out the missing entire, and subsequently fed into the Echo State Network to discover causal relationships among the variables.

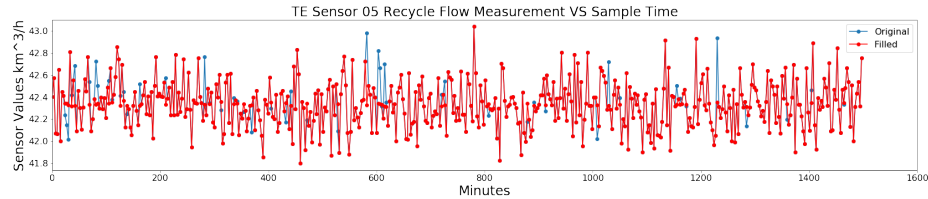


Fig. 4: Original Data VS 10% GPR Filled Data

The process is repeated on three other off-the-shelf causal discovery algorithms, namely:

- Structural Expectation Maximization (SEM) [29]: a graphical approach that is capable of learning causal relationships from sparsely sampled time series data; as

such, the GPR process is not used for this algorithm, and the missing data are directly fed into the SEM algorithm for causal learning. We report on the results of *bnstruct* [43], an R implementation of SEM.

- Subsampled Linear Auto-Regression Absolute Coefficients algorithm (SLARAC): a classical approach for causal discovery written in python, and can be found at [9].
- Multivariate Granger Causality (MVGC): a classical approach written in Matlab and can be found at [11].

The GPR filling is applied to both classical approaches before performing causal discovery. To validate the impact of the data filling process, we also include our results obtained from then ESN with the original data (no missing values).

The experimental comparison setup for the various systems is summarized in Fig. 5.

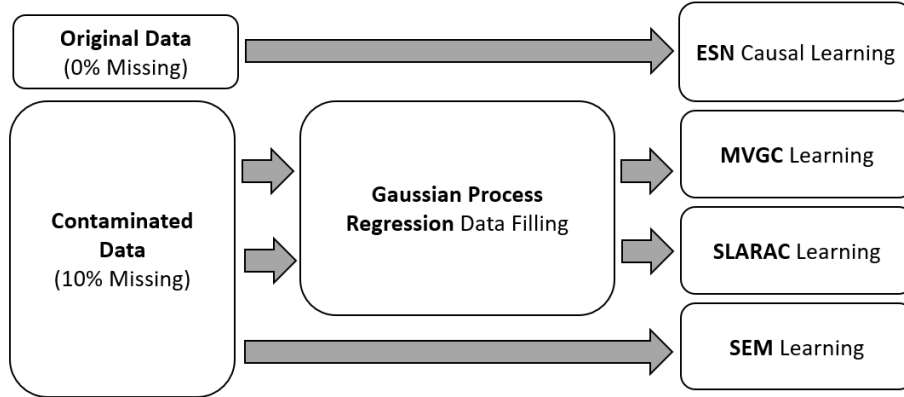


Fig. 5: The Proposed Experiment Setup for Performance Comparison.

4.3 Evaluation Metrics

We validate the performance of the various systems using the Matthews Correlation Coefficient (MCC) score:

$$\text{MCC} = \frac{TP \times TN - FP \times FN}{\sqrt{(TP + FP)(TP + FN)(TN + FP)(TN + FN)}}, \quad (17)$$

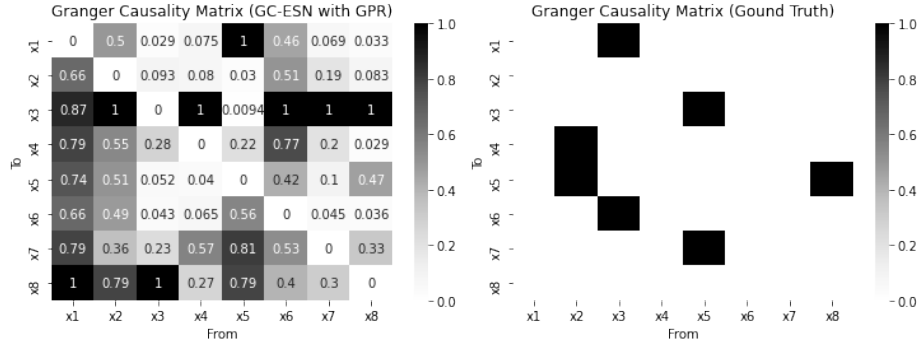
that reflects the *usefulness* of each causal prediction. The MCC score provides a balanced measure between the True Positive (TP), True Negative (TN), False Positive (FP) and False Negative (FN) cases; its output is $\in [-1, 1]$, where a 1 score indicates a perfect prediction, 0 indicates that the prediction made is no better than random guessing, and -1 indicates complete disagreement between prediction and observation [44].

In addition to the MCC index comparison, we also report on the ROC (Receiver Operating Characteristic) curves for the various causal discovery systems. The ROC

curves offer valuable insights into the specificity and sensitivity of each model at different cutoff thresholds in the causal matrices. We also report on the AUC (Area Under Curve) score for all ROC curves. Note that due to the binary matrix output nature of the SEM algorithm, we were unable to plot its ROC curve.

4.4 Results and Discussion

Figure 6 shows the causal relations recovered from our proposed GC-ESN system (a) side-by-side with its corresponding ground truth causality matrix (b). On the other hand, table 2 summarizes the MCC index of the proposed system (GPR + ESN 10% Missing) against the other algorithms.



(a) Causal Matrix of GC-ESN with 10% GPR (b) The Ground Truth Causal Matrix

Fig. 6: Causal Matrix Comparison between GC-ESN with 10% Missing Data Filling using GPR and the Ground Truth.

Table 2: MCC Score Results

	GC-ESN 0% Missing	GPR + GC-ESN 10% Missing	GPR + SLARAC 10% Missing	MVGC 10% Missing	SEM 10% Missing
TP	5	5	7	7	0
FP	13	15	47	48	13
TN	44	42	8	9	44
FN	2	2	0	0	7
MCC	0.34	0.31	0.15	0.14	-0.18

As shown in Table. 2, our system was capable of recovering five of the seven causal relations by applying thresholds that yield the highest F1 scores, and despite the 10 % missing entries, our proposed system still achieved an MCC index (Table 2) of 0.31

which is slightly lower (by 0.03) than the MCC index obtained with the original data (using ESN causal learning). This indicates that the GPR filling process we adapted inside our system is very effective and did restore a satisfactory amount of information comparable to that of the original data. Furthermore, compared to the remaining algorithms on missing data, the proposed GC-ESN estimator achieved the highest MCC score. This indicates that our proposed system is capable of offering more precise and reliable causal links suggestions than the other systems.

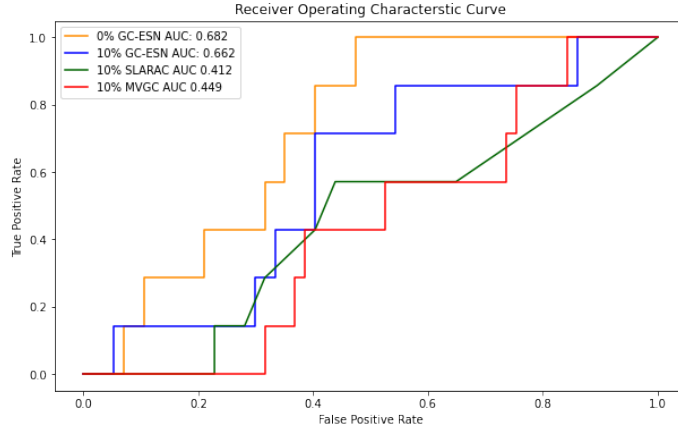


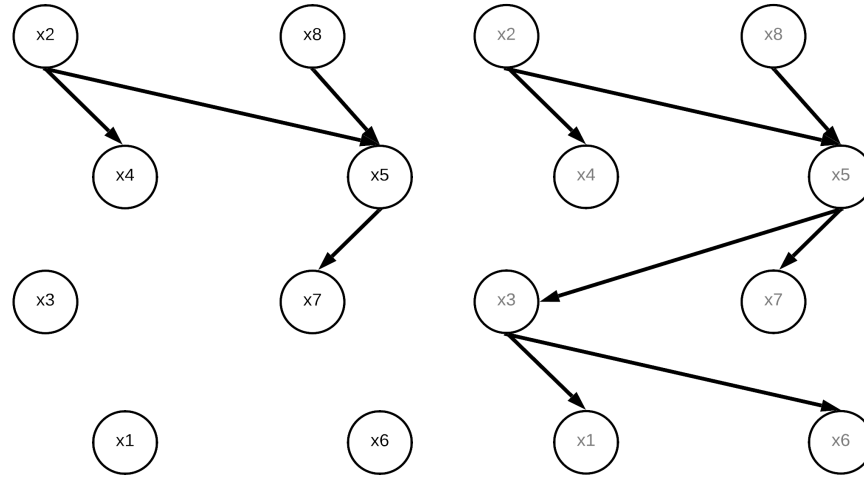
Fig. 7: ROC Curve for Different Missing Percentage GC-ESN and other estimators. The proposed system is able to outperform the rest of the estimators by a noticeable margin in their AUC scores.

The results of the ROC curves (shown in Fig. 7) further solidify our claims as our proposed GC-ESN system reports a significantly larger AUC score than the rest (other than ESN on the original data). Moreover, by varying the threshold values, GC-ESN has the highest true positive rate, proving that among the three estimators, GC-ESN exhibits the best performance.

Figure 8 shows the results from Figure 6 using causal diagram. Different colours represent different causal features and different thicknesses of connections represent different weights. It is consistent with the comparison results from Figure 7.

5 Conclusion

We have proposed a system capable of performing causal discovery for sparsely sampled multivariate time series data. The system consists of two parts: (1) Data filling with Gaussian Process Regression, and (2) causal learning with an Echo State Network. The proposed system is evaluated on the Tennessee Eastman (TE) process dataset with 10 percent missing entries. In order for us to evaluate the performance, the proposed system is compared and shown to outperform several other methods including Structural



(a) Causal Diagram of GC-ESN with 10% GPR (b) The Ground Truth Causal Diagram

Fig. 8: Results Comparison between GC-ESN (true positive) with 10% missing data by applying a 0.5 threshold value filling using GPR and the Ground Truth, we are able to obtain 4 true positive causal relations out of 7 which is better than result obtained from other methods.

Expectation Maximization (SEM), Subsampled Linear Auto-Regression Absolute Coefficients (SLARAC), and Multivariate Granger Causality (MVGCC).

We also perform an ablation study to evaluate the effectiveness of the GPR in recovering causal information by comparing its results to that of causal discovery using the original (uncontaminated) data, and found that the proposed data filling process is capable of recovering causal relationships reliably and performed only marginally worse had the full original data was used. This work shows promise in recovering causal relationships from imperfect data better than current SOTA (State Of The Art) methods.

The obtained results show great potential in applying the proposed system in more complicated real world scenarios as it outperforms all other methods by a comfortable margin in both AUC scores and MCC indices.

That being said, the proposed system still fall short in comparison to a human subject-expert in identifying causal relationships; as such, causal discovery remains an ongoing research topic.

Acknowledgements

We would like to thank the Ontario Centres of Excellence (OCE), Natural Sciences and Engineering Research Council (NSERC) and ATS Automation Tooling Systems Inc., for supporting this research work.

Bibliography

- [1] J. Pearl, Theoretical impediments to machine learning with seven sparks from the causal revolution, CoRR abs/1801.04016 (2018). [arXiv:1801.04016](https://arxiv.org/abs/1801.04016).
- [2] P. L. Bartlett, A. Montanari, A. Rakhlin, Deep learning: a statistical viewpoint, arXiv preprint arXiv:2103.09177 (2021).
- [3] M. Hernán, B. Brumback, J. Robins, Marginal structural models to estimate the causal effect of zidovudine on the survival of hiv-positive men., *Epidemiology* 11 5 (2000) 561–70.
- [4] J. Hicks, et al., *Causality in economics*, Australian National University Press, 1980.
- [5] J. J. Heckman, *Econometric causality*, *International statistical review* 76 (1) (2008) 1–27.
- [6] R. P. Thompson, *Causality, mathematical models and statistical association: dismantling evidence-based medicine*, *Journal of Evaluation in Clinical Practice* 16 (2) (2010) 267–275.
- [7] R. Guo, L. Cheng, J. Li, P. R. Hahn, H. Liu, A survey of learning causality with data, *ACM Computing Surveys* 53 (4) (2020) 1–37. doi:10.1145/3397269.
- [8] L. Yao, Z. Chu, S. Li, Y. Li, J. Gao, A. Zhang, A survey on causal inference (2020). [arXiv:2002.02770](https://arxiv.org/abs/2002.02770).
- [9] S. Weichwald, M. E. Jakobsen, P. B. Mogensen, L. Petersen, N. Thams, G. Varando, Causal structure learning from time series: Large regression coefficients may predict causal links better in practice than small p-values, in: H. J. Escalante, R. Hadsell (Eds.), *Proceedings of the NeurIPS 2019 Competition and Demonstration Track*, Vol. 123 of *Proceedings of Machine Learning Research*, PMLR, 2020, pp. 27–36.
URL <http://proceedings.mlr.press/v123/weichwald20a.html>
- [10] M. Nauta, D. Bucur, C. Seifert, Causal discovery with attention-based convolutional neural networks, *Machine Learning and Knowledge Extraction* 1 (1) (2019) 312–340. doi:10.3390/make1010019.
- [11] L. Barnett, A. K. Seth, The mvgc multivariate granger causality toolbox: A new approach to granger-causal inference, *Journal of Neuroscience Methods* 223 (2014) 50–68. doi:<https://doi.org/10.1016/j.jneumeth.2013.10.018>.
- [12] B. Chang, M. Naiel, S. Wardell, S. Kleinikink, J. Zelek, Time-series causality with missing data, *Journal of Computational Vision and Imaging Systems* 6 (1) (2021) 1–4. doi:10.15353/jcvis.v6i1.3552.
URL <https://openjournals.uwaterloo.ca/index.php/vs1/article/view/3552>
- [13] C. W. J. Granger, Investigating causal relations by econometric models and cross-spectral methods, *Econometrica* 37 (3) (1969) 424–438.
URL <http://www.jstor.org/stable/1912791>

- [14] J. Goldstein, Causality and emergence in chaos and complexity theories, in: *Non-linear dynamics in human behavior*, World Scientific, 1996, pp. 159–190.
- [15] P.-O. Amblard, O. J. Michel, The relation between granger causality and directed information theory: A review, *Entropy* 15 (1) (2013) 113–143.
- [16] R. Dahlhaus, M. Eichler, *Causality and graphical models in time series analysis*, Oxford Statistical Science Series (2003) 115–137.
- [17] B. Schölkopf, *Causality for machine learning*, arXiv preprint arXiv:1911.10500 (2019).
- [18] H. Y. Toda, P. C. B. Phillips, Vector autoregressions and causality, *Econometrica* 61 (6) (1993) 1367–1393.
URL <http://www.jstor.org/stable/2951647>
- [19] K. Mainali, S. Bewick, B. Vecchio-Pagan, D. Karig, W. F. Fagan, Detecting interaction networks in the human microbiome with conditional granger causality, *PLoS computational biology* 15 (5) (2019) e1007037.
- [20] Z. He, K. Maekawa, On spurious granger causality, *Economics Letters* 73 (3) (2001) 307–313.
- [21] H. Y. Toda, T. Yamamoto, Statistical inference in vector autoregressions with possibly integrated processes, *Journal of Econometrics* 66 (1) (1995) 225–250.
doi:[https://doi.org/10.1016/0304-4076\(94\)01616-8](https://doi.org/10.1016/0304-4076(94)01616-8).
- [22] E. G. Baek, W. A. Brock, A nonparametric test for independence of a multivariate time series, *Statistica Sinica* 2 (1) (1992) 137–156.
- [23] G. Sugihara, R. May, H. Ye, C.-h. Hsieh, E. Deyle, M. Fogarty, S. Munch, Detecting causality in complex ecosystems, *Science* 338 (6106) (2012) 496–500.
doi:[10.1126/science.1227079](https://doi.org/10.1126/science.1227079).
- [24] P. Duan, F. Yang, T. Chen, S. L. Shah, Direct causality detection via the transfer entropy approach, *IEEE transactions on control systems technology* 21 (6) (2013) 2052–2066.
- [25] F. Yang, P. Duan, S. L. Shah, T. Chen, *Capturing connectivity and causality in complex industrial processes*, Springer Science & Business Media, 2014.
- [26] R. Bishop, Chaos, in: E. N. Zalta (Ed.), *The Stanford Encyclopedia of Philosophy*, spring 2017 Edition, Metaphysics Research Lab, Stanford University, 2017, pp. ..
- [27] J. Runge, P. Nowack, M. Kretschmer, S. Flaxman, D. Sejdinovic, Detecting and quantifying causal associations in large nonlinear time series datasets, *Science Advances* 5 (11) (2019) eaau4996. doi:[10.1126/sciadv.aau4996](https://doi.org/10.1126/sciadv.aau4996).
- [28] M. Gong, K. Zhang, B. Schoelkopf, D. Tao, P. Geiger, Discovering temporal causal relations from subsampled data, in: *International Conference on Machine Learning*, PMLR, 2015, pp. 1898–1906.
- [29] N. Friedman, *The bayesian structural em algorithm* (2013). arXiv:1301.7373.
- [30] H. Nikpour, A. Aamodt, K. Bach, Bayesian-supported retrieval in bncreek: A knowledge-intensive case-based reasoning system, in: M. T. Cox, P. Funk, S. Begum (Eds.), *Case-Based Reasoning Research and Development*, Springer International Publishing, Cham, 2018, pp. 323–338.
- [31] H. Jaeger, The “echo state” approach to analysing and training recurrent neural networks, GMD-Report 148, German National Research Institute for Computer Science (01 2001).

- [32] O. Biran, C. Cotton, Explanation and justification in machine learning: A survey, in: IJCAI-17 workshop on explainable AI (XAI), Vol. 8, 2017, pp. 8–13.
- [33] A. Duggento, M. Guerrisi, N. Toschi, Echo state network models for nonlinear granger causality, *bioRxiv* (2019). arXiv:<https://www.biorxiv.org/content/early/2019/05/27/651679.full.pdf>, doi:10.1101/651679.
URL <https://www.biorxiv.org/content/early/2019/05/27/651679>
- [34] C. E. Rasmussen, C. K. I. Williams, *Gaussian Processes for Machine Learning (Adaptive Computation and Machine Learning)*, The MIT Press, 2005.
- [35] J. Bernardo, J. Berger, A. Dawid, A. Smith, et al., Regression and classification using gaussian process priors, *Bayesian statistics* 6 (1998) 475.
- [36] F. Jäkel, B. Schölkopf, F. Wichmann, A tutorial on kernel methods for categorization, *Journal of Mathematical Psychology* 51 (6) (2007) 343–358.
- [37] E. Schulz, M. Speekenbrink, A. Krause, A tutorial on gaussian process regression: Modelling, exploring, and exploiting functions, *Journal of Mathematical Psychology* 85 (2018) 1 – 16.
- [38] H. Jaeger, *Short term memory in echo state networks*, Vol. 5, GMD-Forschungszentrum Informationstechnik, 2001.
- [39] X. Chen, Tennessee eastman simulation dataset (2019). doi:10.21227/4519-z502.
URL <https://dx.doi.org/10.21227/4519-z502>
- [40] X. Chen, J. Wang, J. Zhou, Probability density estimation and bayesian causal analysis based fault detection and root identification, *Industrial & Engineering Chemistry Research* 57 (43) (2018) 14656–14664. doi:10.1021/acs.iecr.8b03009.
- [41] H. Gharahbagheri, S. A. Imtiaz, F. Khan, Root cause diagnosis of process fault using kpca and bayesian network, *Industrial & Engineering Chemistry Research* 56 (8) (2017) 2054–2070. doi:10.1021/acs.iecr.6b01916.
- [42] C. A. Rieth, B. D. Amsel, R. Tran, M. B. Cook, Issues and advances in anomaly detection evaluation for joint human-automated systems, in: J. Chen (Ed.), *Advances in Human Factors in Robots and Unmanned Systems*, Springer International Publishing, Cham, 2018, pp. 52–63.
- [43] A. Franzin, F. Sambo, B. di Camillo, bnstruct: an r package for bayesian network structure learning in the presence of missing data, *Bioinformatics* 33 (8) (2017) 1250–1252. doi:10.1093/bioinformatics/btw807.
- [44] B. Matthews, Comparison of the predicted and observed secondary structure of t4 phage lysozyme, *Biochimica et Biophysica Acta (BBA) - Protein Structure* 405 (2) (1975) 442–451.